Appl. Phys. B 53, 34–38 (1991)

Applied Physics B Photophysics and Laser Chemistry

Observations and Analysis of Resonant Laser Ablation of GaAs

L. Wang[1,*], I. S. Borthwick[1], R. Jennings[1], P.T. McCombes[1], K.W.D. Ledingham[1], R.P. Singhal[1], and C.J. McLean[2]

[1] Department of Physics and Astronomy, University of Glasgow, Glasgow G12 8QQ, UK
[2] Department of Electronics and Electrical Engineering, University of Glasgow, Glasgow G12 8QQ

Received 29 October 1990/Accepted 6 April 1991

Abstract. Laser ablation of solid GaAs samples has been studied using one tunable pulsed dye laser. At relatively low laser power, enhancements of up to several hundred times have been observed in the yield of resonantly ionised Ga using laser wavelengths corresponding to the atomic transition $4^2P_{1/2}$–$4^2D_{3/2}$. The influences of laser power and target geometry, on the ion yield and spectral profile, are discussed. It is argued that the resonant excitation and ionisation processes occur in the gas phase of the atoms ablated from the sample surface, and the observed asymmetric spectral profile results from laser-induced collisional processes, e.g., optical collisions, under conditions of relatively high atomic density in the interaction region. Potential applications are foreseen for resonant laser ablation in trace analysis.

PACS: 32.80, 32.90.+1, 79.20.Ds

Laser ablation has been used extensively to vaporise target materials and has given rise to the analytical instruments LIMA [1] and LAMMA [2], which typically use a quadrupled Nd:YAG laser in conjunction with a reflectron time-of-flight mass spectrometer to analyse the ions produced in the ablation process. It is believed that the ion yield is dominated by plasma processes, and that in most cases the yield of ions is several orders of magnitude lower than that of neutrals, estimated by the Saha equation [3]. Thus greater sensitivity can be achieved by efficiently ionising the ablated neutral species with a delayed laser pulse tuned to a resonant transition wavelength of the specific atoms. This is the basis of one of the variants of resonant ionisation mass spectrometry (RIMS) [4], namely laser ablation with resonant post ablation ionisation.

Recent studies [5, 6] have indicated that both ablation and resonant ionisation may be performed with a single tunable laser pulse to provide resonant enhancements of the ion yield of up to 70 times. Considerable broadening of the resonant signals ($\sim$1 nm) was observed in both studies, where the ablating laser was directed normally onto the sample, in transmission mode in one case [5] and in conjunction with 50 Torr of He buffer gas in the other [6]. In a recent paper McLean et al. [7] have shown that if a moderately focused resonant laser beam is directed at grazing incidence to the target, signal enhancements of greater than two orders of magnitude can be obtained. In addition, the resonant widths are less than 0.05 nm at wavelengths corresponding to known atomic transitions. In light of these observations, and in view of their considerable potential in the analysis of solid samples, a detailed study of grazing-incidence resonant laser ablation was undertaken.

1. Instrumentation

The mass spectrometer used for the ablation studies is shown in Fig. 1, and comprised an analysis chamber, an entry chamber for rapid transfer of samples, and a one metre linear time-of-flight mass analyser of mass resolution approximately 100. The operational pressure was typically $\sim 10^{-8}$ mbar and the ion detector an electron multiplier. The GaAs sample was mounted on a 25 mm diameter stainless steel stub and fixed with conductive epoxy.

The laser arrangement consisted of a Lumonics TE 860-3 XeCl (308 nm) pumping a Lumonics EPD 330 dye laser employing Rhodamine 6G. The dye laser output was frequency doubled using a KDP crystal mounted on an Inrad autotracker. The pulse length was 5 ns and the bandwidth $\sim$0.01 nm.

* Permanent address: Institute of Physics, Chinese Academy of Sciences, P.O. Box 603, Beijing, P.R. China

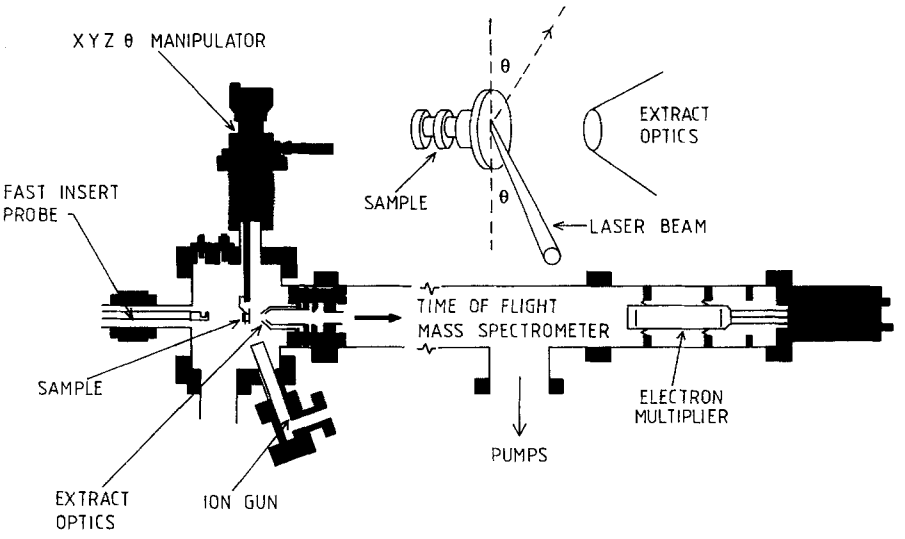

Fig. 1. Time of flight mass spectrometer system showing grazing angle θ of incident laser beam

The data acquisition system, which consisted essentially of a 12-bit Ortec AD811 peak sensing ADC with a gate of variable width and delay coupled to an LSI-11 microprocessor, has been described in detail elsewhere [8].

2. Results and Discussion

A GaAs sample with a smooth mirror finish was used in these experiments. The target geometry is shown in Fig. 1. Both the fundamental and frequency-doubled laser beam components were directed at grazing incidence to the surface, and moderately focused by a quartz lens ($f=50$ cm) to give a beam diameter of 0.5 mm. The left inset in Fig. 2 is a partial Grotrian diagram of Ga showing the states involved in the excitation and ionisation processes of the experiments. The ultraviolet (UV) output was tuned to around the $4^2P_{1/2}$–$4^2D_{3/2}$ transition (287.5 nm) of Ga and the further absorption of a fundamental photon resulted in ionisation of the excited atoms. The total laser intensity onto the surface (area ~ 2.5 mm) of the sample was typically $\leqq 8\times10^6$ Wcm^{-2}, of which the UV component was about 20%.

2.1 Effects of Laser Intensity on Ionisation Spectra

The grazing incident angle on the sample was fixed at 5°, and the total laser pulse energy was varied from the ion detection threshold up to 1 mJ. Over this energy range, the time-of-flight ion signals were very clear and the two isotopes of gallium, ^{69}Ga and ^{71}Ga, were well resolved. At each energy a wavelength scan was obtained. The spectra are shown in Fig. 2, and a resonant enhancement of several hundred is clearly seen. Due to the resonantly enhanced excitation, the ion yield is increased and therefore the ejected particles were detected with a lower laser fluence than required in the case of non-resonant ablation. As the laser energy increases, the resonant width increases asymmetrically towards longer wavelengths.

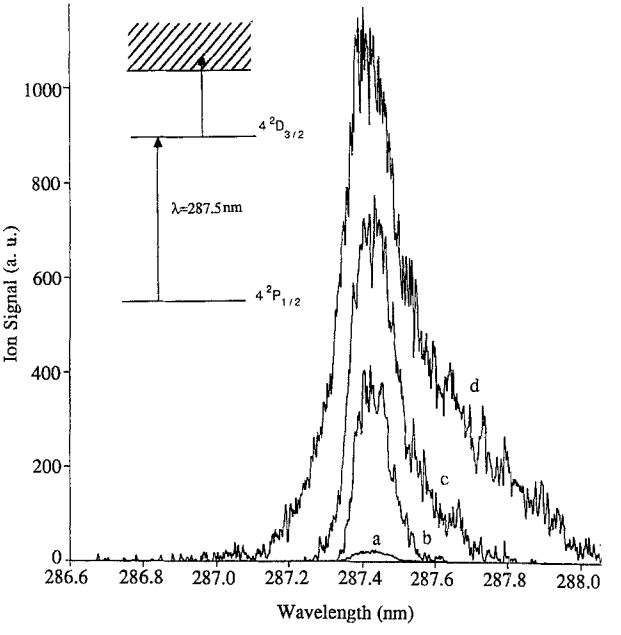

Fig. 2. The ion signal of Ga as functions of UV laser wavelength λ, and total laser energy E. The grazing incident angle of the laser beam onto the sample surface is $\theta=5°$. The corresponding total ablation energy is (a) $E=0.39$ mJ, (b) $E=0.66$ mJ, (c) $E=0.79$ mJ, and (d) $E=0.98$ mJ. The resonant enhancement can be clearly seen with the resonant width increasing asymmetrically as the laser energy increases. The left inset is a partial Grotrian diagram of Ga relevant to the experiments

When the laser energy was further increased, the dramatic resonance disappeared and the resolution of the time-of-flight mass spectra became poor due to space charge effects and the probable onset of plasma processes in the ablated plume.

At relatively low pulse energies the spectral profiles had widths of about 0.1 nm and were centered at the corresponding atomic transition $4^2P_{12}-4^2D_{3/2}$ calibrated using a uranium/argon hollow cathode lamp. The sharp resonance indicated that the neutrals were first desorbed

from the surface of the sample, resonantly excited, and then subsequently ionised in the gas phase by the same laser pulse. This is a two-step process which is quite different from that using a non-resonant laser of high power, as for example in LIMA and LAMMA, where ions are produced predominantly by plasma reactions, and the ablation and ionisation processes cannot be entirely separated spatially and temporally. The processes here are thus very similar to the resonant post-ablation ionisation involving two lasers.

The wide and asymmetric profiles of the resonances shown in Fig. 2 require careful consideration. A possible model of the physical process occurring within the short duration of the laser pulse (~ 5 ns), which might lead to the observed spectral shapes is as follows.

a) The laser initially ablates the sample creating neutrals, a process which is independent of wavelength over the range studied here.

b) The main contribution to the observed spectral width arises from the large value of the Rabi frequency (power broadening). The $4^2P_{1/2} \rightarrow 4^2D_{3/2}$ transition probability is $1.2 \times 10^8\ s^{-1}$ [9], corresponding to a Rabi frequency (Ω) of about 1000 GHz for a monochromatic UV laser flux of $10^6\ Wcm^{-2}$ and somewhat lower for a finite bandwidth laser. This is consistent with the observed profiles. Taking into account the short duration of the laser light and the average velocity of the particles leaving the surface of the sample (several hundred ms^{-1}) [10], the interaction of the laser beam with the neutral atoms occurs within a few μm from the surface. If it is assumed that 10^{10} atoms were ablated by a laser pulse of flux $10^6\ Wcm^{-2}$ [11] and taking the irradiated surface area to be 2.5 mm^2, an atomic density of about $10^{15}\ cm^{-3}$ in the interaction region is estimated. Given this atomic density, collisions modify the atomic energy levels, such that a range of transition energies are possible. The asymmetry can be attributed to atomic collisions in the intense laser field, especially to "optical collisions" [12, 13] in the present experiment.

c) These excited atoms can then be either photionised or ionised by energy pooling collisions. The latter process [14–16] has been studied extensively and have been shown to occur with large probability at similar atomic densities to those estimated to the present experiment. In particular, the population of an autoionisation state of indium atoms through inelastic collisions between excited atoms has been reported recently [16]. However, due to the limited experimental data available at present, no firm conclusion can yet be drawn as to which process, photoionisation or collision-assisted ionisation, is the main contribution to ion formation in RLA. It is undoubtedly a question worthy of further study.

Additionally, the asymmetry was found to increase rapidly with the laser intensity. This can also be explained on the basis of the proposed model since the density of ablated neutrals increases strongly with laser fluence.

2.2 *Effects of Target Geometry*

To investigate the effects of target geometry on RLA, the laser pulse energy was kept at fixed values, while a wavelength scan of the ion signal was recorded at angles between 5° and 8°, selected by rotation of the precision manipulator. Owing to the constant conditions for optical excitation and ionisation of the ablated atoms, the net effects on the atomisation process of varying the incident angle can be observed. Larger variation of the incident angle was not explored due to the uncertainties in the extraction efficiency of the mass spectrometer, caused by the distortion of the extraction fields.

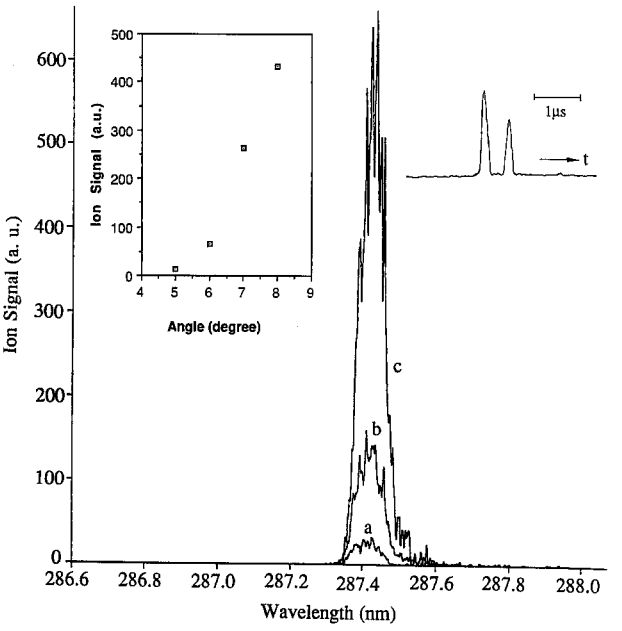

Fig. 3. RLA spectra of Ga at relatively low laser energy, $E = 0.26$ mJ, with different incident angles of laser beam: (a) $\theta = 5°$, (b) $\theta = 6°$, and (c) $\theta = 7°$. The results show strong θ dependence for the ion yield. Upper right insert is the Ga^+ time of fight showing the two isotopes ^{69}Ga and ^{71}Ga well resolved

Figure 3 shows the spectra obtained at a total laser energy $E = 0.26$ mJ (UV energy 56 μJ) while Fig. 4 was recorded at $E = 0.61$ mJ (UV energy 110 μJ). The right inset in Fig. 3 is the Ga^+ time of flight signal showing the two isotopes ^{69}Ga and ^{71}Ga well resolved.

At larger grazing incident angles the laser fluence onto the surface of the sample is higher due to the reduced irradiation area. Simultaneously, more of the incident laser energy is channelled into the solid sample due to the monotonic increase in the transmission factor $1 - R(\theta)$ as θ increases (R is the reflectivity of the ample surface). Together these result in the marked increases in ion yield which were obtained at relatively large incident angles. At low pulse energy (Fig. 3) the peaks remain narrow as θ increases but at high energy (Fig. 4) the peaks become broad asymmetrically towards longer wavelengths, just as in Fig. 2. This observation supports the view that the optical collisions provide an important contribution to ion formation in the spectral wing, and the asymmetrical profile results from an increasing density of the neutrals near the surface of the sample.

Figure 5 shows the result of varying both the laser energy E, and incidence angle θ such that the fluence onto

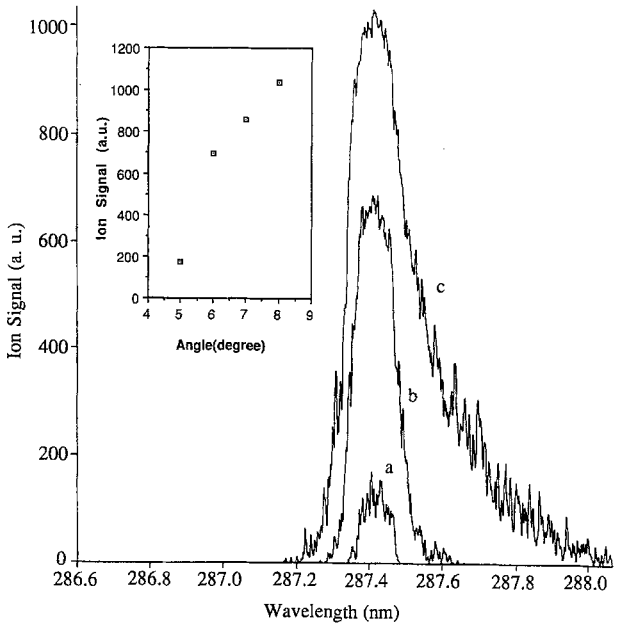

Fig. 4. RLA spectra of Ga at slightly higher laser energy, $E=0.61$ mJ, with different incident angles: (a) $\theta=5°$, (b) $\theta=6°$, and (c) $\theta=8°$. In comparison with Fig. 3, broadening occurs at larger incident angles

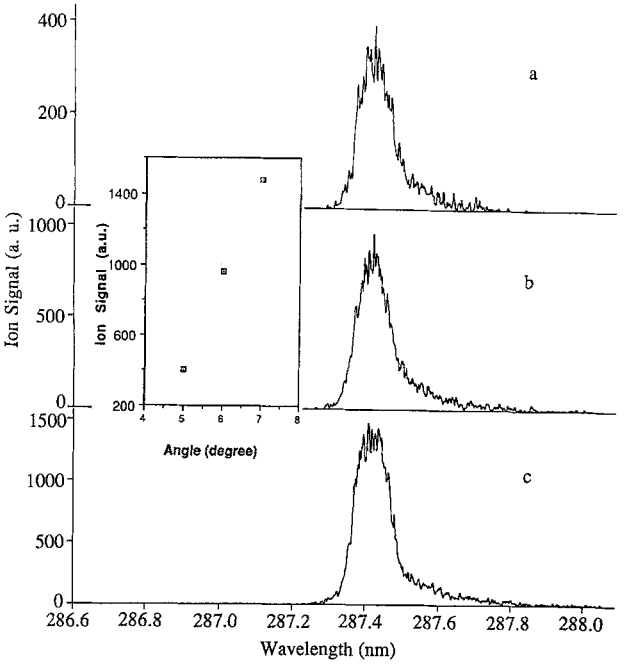

Fig. 5. RLA spectra of Ga with laser fluence kept constant by holding $E\sin\theta=$ constant for different laser energies E and incident angles θ: (a) $E=0.51$ mJ, $\theta=5°$, (b) $E=0.43$ mJ, $\theta=6°$, and (c) $E=0.39$ mJ, $\theta=7°$. The increase in ion signal for large θ is believed to be due to the decreasing reflectivity of the sample surface

the surface of the sample was kept constant (i.e., $E\sin\theta$ = constant), and the ion signal was again plotted as a function of wavelength. In this case, the reduced reflectivity is the only factor accounting for the increased neutral yield at larger incident angles. The ion yield still increased with increasing angle although both the laser energy and the irradiation area on the surface were reduced. This illustrates again the importance of high atomic density in the interaction region for the total ion yield.

The reflectivity determines how much laser energy is transmitted into the solid sample, i.e., the effective ablation intensity. In the interaction of the laser pulse with the atoms of the gas phase following ablation, the effective laser fluence for excitation and ionisation processes is proportional to $(1+R)$. The total ion yield depends on both the neutral density and the excitation-ionisation probability, and can be maximised at constant laser power by choosing a suitable incident angle to provide an optimal ratio of the transmitted and reflected portions of the incident laser energy. In the present experiment, the observed ion yield increased monotonically with the increasing incident angle, which indicates that the ion yield relies more on the density of the neutrals, i.e., ablation yield, than on the photo-ionisation probability (the excitation step was saturated for the laser intensity used in these experiments).

3. Conclusions

Resonant laser ablation has been investigated at different powers and grazing incident angles for Ga from a GaAs sample. The experimental results show that the resonant excitation and subsequent ionisation occur in the gas phase of the atoms produced by laser ablation. At grazing incidence resonant enhancements of several hundred can be obtained with modest laser power. The widths of the profiles are fairly narrow at low laser fluence but increase with both fluence and incident angle, and at high fluences tend to approach the values reported in [5 and 6], where the normal incident configuration must produce more neutrals near the sample surface, resulting in broad resonant peaks. This large width is mainly due to power broadening in the present experiments. The asymmetric profile of the resonant peak is attributed to optical collisions arising from the high density of neutrals near the sample surface. Further studies of the role of collisional processes between excited atoms are in progress.

We believe that the efficient utilisation of the ablated atoms is a unique advantage offered by the resonant laser ablation technique. If the ionisation efficiency is high enough, it is expected to be a potential candidate for trace analysis. The work described in this paper was carried out on Ga, a major constituent of GaAs. Further work is at present being carried out on RLA of trace atomic levels of gold in copper matrices to determine the sensitivity of RLA in comparison with resonant ionisation mass spectrometry. In addition, the importance of RLA may be greater in connection with molecular detection because the parent ions as opposed to fragment ions may be preferentially produced at relatively low laser power by RLA.

Acknowledgements. L.W. wishes to thank the Royal Society for a fellowship while I.S.B., P.T.McC. and C.J.McL. acknowledge receipt of SERC research studentships. K.W.D.L. wishes to thank Dr. M. Towrie (Rutherford Laboratory) for bringing to his attention the topic of photon-assited collisions.

References

1. M.J. Southon, M.C. Witt, E.R. Wallach, J. Myatt: Vacuum **34**, 903–909 (1984)
2. G. Krier, F.R. Verdun, J.F. Muller: Fresenius Z. Anal. Chem. **322**, 379–382 (1985)
3. N. Fürstenau: Fresenius Z. Anal. Chem. **308**, 201–205 (1981)
4. M. Towrie, S.L.T. Drysdale, R. Jennings, A.P. Land, K.W.D. Ledingham, P.T. McCombes, R.P. Singhal, M.H.C. Smyth, C.J. McLean: Int. J. Mass Spectrom. Ion Proc. **96**, 309–320 (1990)
5. F.R. Verdun, G. Krier, J.F. Muller: Anal. Chem. **59**, 1383–1387 (1987)
6. Ho-ming Pang, E.S. Yeung: Anal. Chem. **61**, 2546–2551 (1989)
7. C.J. McLean, J.H. Marsh, A.P. Land, A. Clark, R. Jennings, K.W.D. Ledingham, P.T. McCombes, A. Marshall, R.P. Singhal, M. Towrie: Int. J. Mass Spectrom. Ion Proc. **96**, R1–R7 (1990)
8. C. Raine, K.W.D. Ledingham, K.M. Smith: Nucl. Instrum. Methods **217**, 305–310 (1983)
9. NSRDS-NBS 68, NBS Dec. 1980, US Government Printing Office, Washington (1980)
10. B. Schueler, R.W. Odom: J. Appl. Phys. **61**, 4652–4661 (1987)
11. H.F. Arlinghaus, W.F. Calaway, C.E. Young, M.J. Pellin, D.M. Gruen, L.L. Chase: J. Appl. Phys. **65**, 281–289 (1989)
12. A.M.F. Lau: In *Photon-Assisted Collisions and Related Topics*, ed. by N.K. Rahman, C. Guidotti (OPA, Amsterdam, B.V. 1982) pp. 55–90
13. T. Sizer II, M.G. Raymer: Phys. Rev. A **36**, 2643–58 (1987)
14. S. Geltman: Phys. Rev. A **40**, 2301–2308 (1989)
15. C. Gabbanini, S. Gozzini, G. Squadrito, M. Allegrini, L. Moi: Phys. Rev. A **39**, 6148–6153 (1989)
16. P. Bicchi, A. Kopystynska, M. Mcucci, L. Moi: Phys. Rev. A **41**, 5257–5260 (1990)